



# Hepatoprotective effects of phytochemicals berberine and umbelliferone against methotrexate-induced hepatic intoxication: experimental studies and in silico evidence

Abdel-Gawad S. Shalkami<sup>1</sup> · Emad H. M. Hassanein<sup>1</sup> · Ahmed M. Sayed<sup>2</sup> · Wafaa R. Mohamed<sup>3</sup> · Marwa M. Khalaf<sup>3</sup> · Ramadan A. M. Hemeida<sup>1,4</sup>

Received: 19 February 2021 / Accepted: 5 July 2021 / Published online: 13 July 2021  
© The Author(s), under exclusive licence to Springer-Verlag GmbH Germany, part of Springer Nature 2021

## Abstract

Chemotherapeutic drugs are used effectively to manage wide types of malignancies, but their therapeutic use is limited due to their associated hepatic intoxication. The current study sheds light on the effect of phytochemicals berberine (BBR) and umbelliferone (UMB) on methotrexate (MTX)-induced hepatic intoxication. Forty-eight rats were allocated to normal, BBR (50 mg/kg orally for 10 days), UMB (30 mg/kg orally for 10 days), MTX (20 mg/kg at the 5th day), BBR+MTX, and UMB+MTX. With regard to MTX, the results of this investigation reveal potent amelioration of MTX hepatotoxicity by BBR and UMB through reduction of the elevated serum levels of ALT, ALP, AST, and LDH confirmed by the attenuation of histopathological abrasion in liver tissues. BBR and UMB markedly restored antioxidant status. More importantly, BBR resulted in reducing P<sub>38</sub> mitogen-activated protein kinase (P<sub>38</sub>MAPK), nuclear factor kappa-B (NF-κB), and Kelch-like ECH-associated protein 1 (Keap-1) genes and enhanced mRNA expression of Nrf-2 ( $P < 0.05$ ). Interestingly, in silico studies via molecular docking pinpointed the binding modes of BBR and UMB to the binding pocket residues of P<sub>38</sub>MAPK, NF-κB, and Keap-1 and demonstrated a promising inhibition of Keap-1, P<sub>38</sub>MAPK, and NF-κB. BBR and UMB reduced the expression of pro-apoptotic protein Bax and apoptotic protein caspase-3 as well as increased the expression of anti-apoptotic protein Bcl-2. Therefore, BBR and UMB may denote promising therapeutic agents that can avert hepatic intoxication in patients receiving MTX.

**Keywords** Berberine · Umbelliferone · Methotrexate · Hepatotoxicity · P<sub>38</sub>MAPK · Nrf-2 · Apoptosis

## Introduction

Cancer is regarded as the leading cause of mortality worldwide. Chemotherapeutic drugs are used to treat many types of

malignancies, but their therapeutic use is limited due to their side effects (Schmiegelow 2009). Methotrexate (MTX) is well acknowledged as an anti-metabolite chemotherapeutic agent. It is used on a large scale to treat diverse malignancies and non-malignant conditions (Brown et al. 2016; Malaviya 2016). MTX inhibits dihydrofolate reductase enzyme leading to depletion of intracellular stores of tetrahydrofolate. MTX can induce apoptosis interrelated to the production of reactive oxygen species (ROS) (Herman et al. 2005; Spurlock 3rd et al. 2011).

ROS can damage different cellular structures (proteins, DNA, and lipids) and lead to disturbance of the redox status (Muriel and Gordillo 2016). There are several transcription factors that are affected by the redox status, such as nuclear factor kappa-B (NF-κB) that displays a pivotal role in the inflammation in many illnesses. NF-κB is a master controller of the inflammatory process and cell death in different hepatic diseases. Accumulated evidence pointed out that NF-κB was

Responsible Editor: Mohamed M. Abdel-Daim

✉ Abdel-Gawad S. Shalkami  
abdo\_shalkami@azhar.edu.eg

<sup>1</sup> Department of Pharmacology and Toxicology, Faculty of Pharmacy, Al-Azhar University, Assiut Branch, Assiut 71524, Egypt

<sup>2</sup> Biochemistry Laboratory, Chemistry Department, Faculty of Science, Assiut University, Assiut 71515, Egypt

<sup>3</sup> Department of Pharmacology and Toxicology, Faculty of Pharmacy, Beni-Suef University, Beni-Suef 62514, Egypt

<sup>4</sup> Department of Pharmacology and Toxicology, Faculty of Pharmacy, Deraia University, Menia 61768, Egypt

upregulated in the hepatic injury of various etiologies (Ali et al. 2020; Kamel et al. 2020). The  $P_{38}$  mitogen-activated protein kinase ( $P_{38}$ MAPK) is involved in the activation and induction of NF- $\kappa$ B (Luedde and Schwabe 2011; Yang et al. 2014).

Nuclear factor erythroid 2-related factor 2 (Nrf-2) is regarded as the central regulator of cellular responses to oxidative injury. Nrf-2 is a crucial factor for the detoxification in the liver. Under normal conditions, Nrf-2 was tightly bound to its inhibitor, Kelch-like ECH-associated protein 1 (Keap-1), in the cytoplasm. Upon stress, Nrf-2 is released from Keap-1 and translocated to the nucleus and binds to antioxidant responsive elements (AREs) and resulted in the activation of many cytoprotective genes and detoxification enzymes (Bataille and Manautou 2012; Hassanein et al. 2020; Shin et al. 2013). It has been noted that the activation of the Nrf-2 transcription factor is highly valuable and useful in different models of liver injury such as hepatic ischemia-reperfusion (Mahmoud et al. 2019b), alcoholic hepatic injury (Shen et al. 2018), non-alcoholic steatohepatitis (Hosseini et al. 2020), and acetaminophen hepatotoxicity (Lv et al. 2018).

Another point of view is the cross-talk between oxidative stress and apoptosis. Oxidative stress-induced apoptosis is primarily executed by the upregulation of pro-apoptotic Bcl-2-associated X protein (Bax) and downregulation of anti-apoptotic B-cell lymphoma 2 (Bcl-2) proteins. Bax and Bcl-2 belong to the Bcl-2 family, which exerts a pivotal role in the intrinsic apoptotic pathway (Tait and Green 2013; Youle and Strasser 2008). The final pathway leading to apoptosis is the activation of a series of proteases called caspases (Porter and Jänicke 1999). Interestingly, the Bax/Bcl-2 ratio determined the cell apoptosis and well regulation of Bax/Bcl-2 ratio by natural compounds regarded as a reasonable therapeutic target in hepatic diseases of different etiologies (Akanda et al. 2017; Chu et al. 2016; Tsai et al. 2018).

A robust body of evidence lies in treating acute hepatic damage by using compounds of natural origin, which are considered to have a diverse biological activity and are characterized by high efficacy and low toxicity. Antioxidants can reduce the adverse effects of several classical chemotherapeutic drugs through detoxifying ROS (Newman and Cragg 2016; Nobili et al. 2009). Berberine (BBR), an isoquinoline type of alkaloid, is one of the natural compounds of Chinese medicine that exist in several plants (Imenshahidi and Hosseinzadeh 2019). In cell-based systems, BBR markedly reduced NADPH oxidase-dependent cytoplasmic and mitochondrial ROS production (Sun et al. 2017). Umbelliferone (UMB), or 7-hydroxycoumarin, is one of the most common compounds of the coumarin family. It is abundant in several plants such as carrot, bitter orange, and golden apple (Hassanein et al. 2020). Increasing studies have found that UMB exhibits various pharmacological effects, including antioxidant (Germoush et al. 2018; Yin et al. 2018) and anti-inflammatory effects

(Alotaibi et al. 2020; Hosseini et al. 2020). Applicably, these biological activities of BBR and UMB make them a good applicant to be studied in the treatment of liver intoxication induced by MTX. Since  $P_{38}$ MAPKs/NF- $\kappa$ B, Keap-1/Nrf-2, and Bax/Bcl-2/caspase-3 pathways have become a very attractive target for drug activities, the current study focused on examining the contribution of these pathways in the hepatoprotective effects of BBR and UMB.

## Materials and methods

### Drugs and chemicals

Berberine, UMB, reduced glutathione (GSH), Ellman's reagent, and thiobarbituric acid (TBA) were purchased from Sigma-Aldrich (St. Louis, MO, USA). MTX was obtained from Baxter Company. Assay kits for alanine aminotransferase (ALT), alkaline phosphatase (ALP), aspartate aminotransferase (AST), and lactate dehydrogenase (LDH) were purchased from Biodiagnostics Co., (Egypt). RNA extraction and cDNA synthesis kits and PCR primers ( $P_{38}$ MAPK, NF- $\kappa$ B, Keap-1, Nrf-2, and  $\beta$ -actin) were purchased and synthesized from Vivantis Technologies (Malaysia). SYBR green master mix was purchased from Biorline, myBio, (Ireland). Bax (Catalog # PA5-116541), Bcl2 (Catalog # PA5-27094), and caspase-3 (Catalog # PA5-77887) rabbit polyclonal antibodies were purchased from Thermo Fisher Scientific (CA, USA).

### Animal care

Male Wister albino rats, weighing  $180 \pm 200$  g, were purchased from the central animal house, Faculty of Medicine, Assiut University (Assiut, Egypt). Control housing temperatures were maintained at  $25 \pm 2^\circ\text{C}$  with a 12-h light–12-h dark cycle. Water and various diets were given to animals ad libitum. All animal handling and treatments were conducted according to the guidelines of the care and use of laboratory animals approved by the ethical committee of the Faculty of Medicine, Assiut University (License no: 17200074).

### Experimental design

After 14 days of adaptation, animals were randomly allocated into six groups (eight rats per group).

Group I: Rats received vehicle only (1 ml of 1% carboxymethyl cellulose (CMC)) via oral gavage and served as the normal control group.

Group II: Rats received a single oral dose of BBR (50 mg/kg/day) (Almani et al. 2017) suspended in CMC for 10 days (BBR-treated group).

Group III: Rats received a single oral dose of UMB (30 mg/kg/day) (Wang et al. 2015) suspended in CMC for 10 days (UMB-treated group).

Group IV: Rats were injected with MTX in a single i.p. dose of 20 mg/kg (Ali et al. 2017) at the end of the fifth day of the experiment (MTX-treated group) plus 1 ml of CMC orally.

Group V: Rats received both MTX and BBR treatments as previously specified (BBR+MTX-treated group).

Group VI: Rats received both MTX and UMB treatments as previously specified (UMB+MTX-treated group).

After completing the tenth day, rats were anesthetized with ketamine and blood samples were collected directly from the heart. Serum was separated following centrifugation and used for liver function biomarkers. The liver of each rat was removed and rinsed in ice-cold physiological saline. Ten percent (w/v) tissue homogenates were prepared in ice-cooled phosphate-buffered saline (PBS).

## Biochemical investigations

### Assessment of liver enzymes

Measurement of liver enzymes (ALT, AST, ALP, and LDH) was done by commercial kits according to manufacturer instructions. The ALT and AST activities were colorimetrically determined using the kit's principle, which involves measuring the amount of pyruvate or oxaloacetate produced by forming 2,4-dinitrophenylhydrazone (Reitman and Frankel 1957). Belfield and Goldberg (1971) described a method for determining ALP, in which ALP acts on phenyl phosphate and liberates phenol. In the presence of 4-aminophenazone and potassium ferricyanide, the liberated phenol is colorimetrically measured. LDH was measured using the Izquierdo et al. (1982) method, in which LDH catalyzes the reduction of pyruvate by NADH to form lactate and NAD<sup>+</sup>. The rate of decrease of NADH was used to calculate the catalytic concentration.

### Estimation of hepatic oxidative stress parameters

The assay of lipid peroxidation in hepatic tissue was investigated by measurement of MDA level according to the method of Mihara and Uchiyama (1978). Moreover, estimation of GSH content in liver tissue homogenate was described by the method of Ellman (1959), while the hepatic NO was determined by the method of Montgomery and Dymock (1961). Finally, the hepatic activity of SOD is determined according to the method of Marklund and Marklund (1974).

## Gene's expression

Transcription of Keap-1, Nrf-2, P<sub>38</sub>MAPK, and NF- $\kappa$ B genes was analyzed by quantitative real-time polymerase chain reaction (qRT-PCR) in hepatic tissues. Total RNA extraction is done using a kit according to manufacturer instructions. Samples were lysed in the presence of a specially formulated buffer that inactivates cellular RNases. RNA was eluted in RNase-free water. cDNA synthesis was done by using a kit in which reverse transcriptase was used to synthesize first-strand cDNA from 2- $\mu$ g total RNA. mRNA expressions were quantified by qRT-PCR using SYBR green, and then qRT-PCR was performed according to the manufacturer's specifications. As a housekeeping gene, the  $\beta$ -actin is used. After PCR amplification, the  $\Delta\Delta$  Ct was used for calculating by subtraction of the  $\beta$ -actin Ct from each sample Ct (Livak and Schmittgen 2001). The sequences of the primers (Keap-1, Nrf-2, P<sub>38</sub>MAPK, and NF- $\kappa$ B) used are shown in Table 1.

## Histopathological examination

Liver tissue samples were fixed in 10% neutral buffered formalin, dehydrated using alcohol, and embedded in paraffin. Paraffin sections (5- $\mu$ m thickness) were stained with hematoxylin and eosin (H&E) and examined for histopathological changes under the light microscope blind by the method of Bancroft and Gamble (2008). The liver fields were scored according to Derelanko (2008) as follows: normal appearance (-), mild (+), moderate (++) , severe (+++).

## Immunohistochemical analysis

In brief, 5- $\mu$ m-thick paraffin sections were deparaffinized and rehydrated with a series of xylene and alcohol solutions. The deparaffinized hepatic slices were treated with 3% H<sub>2</sub>O<sub>2</sub> for 30 min at 37°C for quenching of endogenous peroxidase activity. The deparaffinized hepatic slices were incubated overnight at 4°C with primary antibodies against Bax (dilution 1:100), Bcl-2 (dilution 1:100), and caspase-3 (dilution 1:100). The sections were rinsed in PBS, incubated in horseradish peroxidase. Slices were conjugated with secondary antibodies for 1 hour at 37°C and rinsed in PBS. Immuno-reactivity was detected using diaminobenzidine, followed by counterstaining with hematoxylin. Slides prepared for each case were examined by light microscopy (Ramos-Vara and Miller 2014). Determination of mean area percentage of Bax, Bcl-2, and caspase-3 immunoreactivity was used for quantification of protein expression from non-overlapping microscopic fields using Leica application software for immune-expression analysis (Leica Biosystems, Germany).

**Table 1** The sequences of the Keap-1, Nrf-2, P<sub>38</sub>MAPK, NF- $\kappa$ B, and  $\beta$ -actin primers

Gene	Primer sequence	Annealing temperature	Product size (bp)	Accession number	Position on the gene	
					Start	Stop
Keap-1	5' TCAGCTAGAGGCGTACTGGA3'	57 °C	500	XM_006242591.3	64	83
	3' TTCGGTTACCATCCTGCGAG5'				563	544
Nrf-2	5' CCGTCCCTAGGTCCTTGTTTC3'	57 °C	619	XM_006234396.3	36	55
	3' CAGGGCAAGCGACTGAAATG5'				654	635
P <sub>38</sub> MAPK	5' AGAGTCTCTGTGCGACCTGCT3'	55 °C	156	XM_017601781.1	1072	1091
	3' CCTGCTTTCAAAGGACTGGT5'				1227	1208
NF- $\kappa$ B	5' TGGGACGACACCTCTACACA3'	55 °C	411	XM_006233360.4	2806	2825
	3' GGAGTCATCTCATAGTTGTCC5'				3250	3229
$\beta$ -actin	5' CCACCATGTACCCAGGCATT3'	55 °C	243	XM_039089807.1	966	985
	3' ACGCAGCTCAGTAACAGTCC5'				1208	1189

### In silico studies

Molecular docking of BBR and UMB against P<sub>38</sub>MAPK, Keap-1, and NF- $\kappa$ B was performed by using AutoDock Vina 1.5.6 (Trott and Olson 2010). The complex

structures of P<sub>38</sub>MAPK, Keap-1, and NF- $\kappa$ B with their binding ligands were retrieved from protein data bank with PDB IDs 3ZS5 (Azevedo et al. 2012), 4L7B (Jnoff et al. 2014), and 1VKX (Chen et al. 1998), respectively. All ligands and water molecules were removed from the

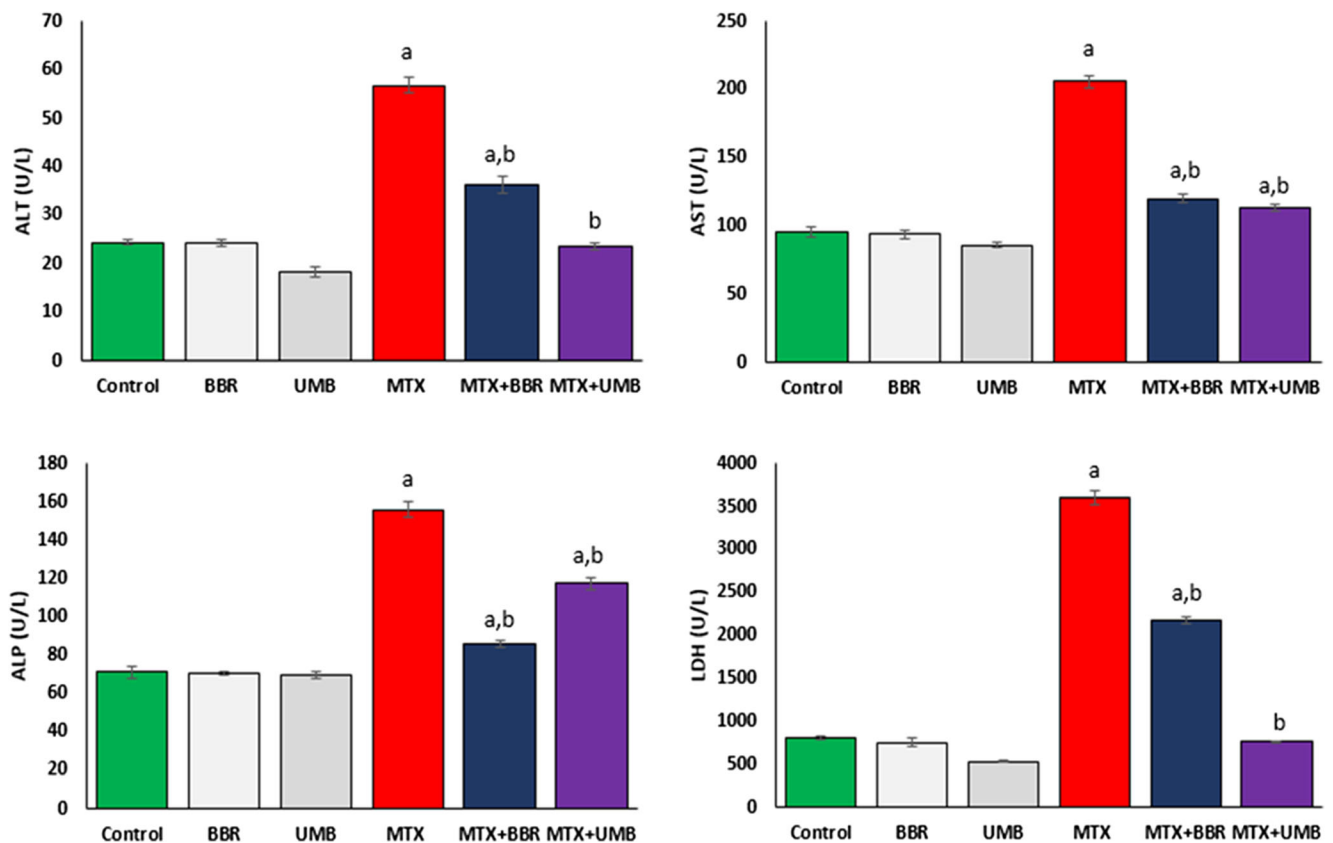


**Fig. 1** Effect of BBR and UMB on serum ALT, ALP, AST, and LDH levels of MTX-intoxicated rats. BBR, berberine; UMB, umbelliferone; MTX, methotrexate; ALT, alanine aminotransferase; AST, aspartate aminotransferase; ALP, alkaline phosphatase; LDH, lactate dehydrogenase. Data were presented as mean of 8 rats  $\pm$  SEM. Statistical analysis was

performed by using one-way ANOVA followed by Tukey's post hoc comparison test. <sup>a</sup>Statistically significant difference from normal control group at  $P < 0.05$ . <sup>b</sup>Statistically significant difference from MTX group at  $P < 0.05$

**Table 2** lesion scores for liver histopathological findings

Histopathological lesion	Control	BBR	UMB	MTX	MTX+BBR	MTX+UMB
Cytoplasmic vacuolization of hepatocytes	–	–	–	+++	+	+
Congestion of hepatic sinusoids	–	–	–	+++	–	–
Kupffer cells activation	–	–	–	++	–	–
Portal inflammatory cells infiltration	–	–	–	+	–	–

–, no change; +, mild change; ++, moderate change; +++, severe change

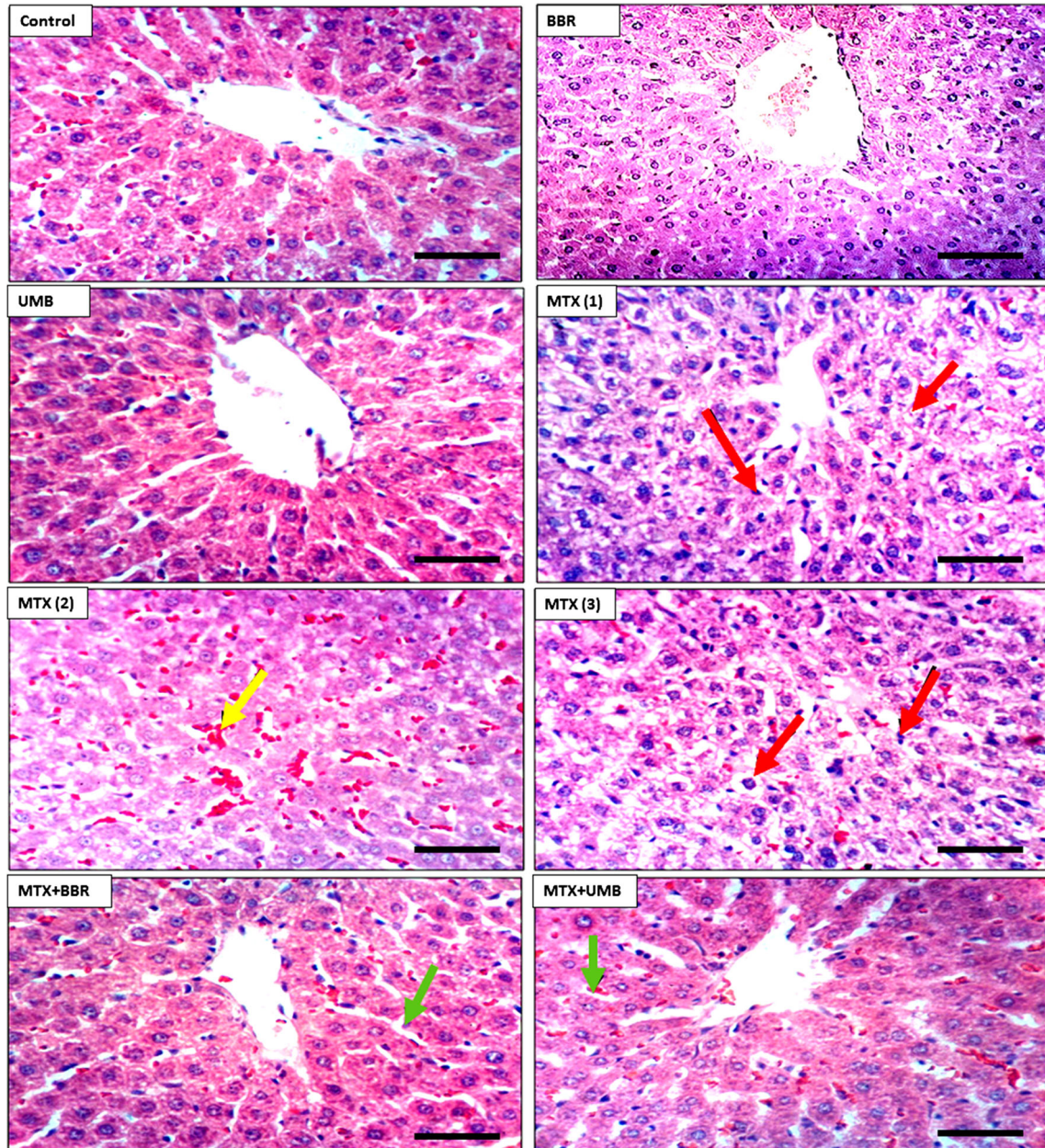


**Fig. 2** Effect of BBR and UMB on hepatic histopathological aberrations induced by MTX. BBR, berberine; UMB, umbelliferone; MTX, methotrexate. Photomicrographs showed that liver section for control and BBR- and UMB-treated groups showed a normal histological structure of hepatic lobule. Sever histopathological changes for rats treated with MTX in the form of a cytoplasmic vacuolization of hepatocytes,

inflammatory cell infiltration (red arrow), and congestion of both central veins and hepatic sinusoids (yellow arrow). An improvement in the histopathological examination resulted from combined administration of BBR or UMB with MTX in liver sections with slight vacuolation of some hepatocytes (green arrow)

complex structures and the PDBQT files were prepared accordingly. Chimera 1.12 software was used to visualize and analyze the binding of berberine and umbelliferone with P<sub>38</sub>MAPK, Keap-1, and NF- $\kappa$ B.

### Statistical analysis

Data obtained were analyzed using SPSS, version 20. Values in the text are the mean  $\pm$  standard error (SEM). One-way analysis of variance (ANOVA) test with Tukey's post hoc comparison test was applied across all groups for testing the significant difference ( $P < 0.05$ ).

## Results

### Effect of BBR and UMB on MTX-induced liver dysfunction in rats

In this work, MTX administration resulted in significant development of hepatic injury as demonstrated by a dramatic rise of serum ALT, ALP, AST, and LDH activities in the MTX-treated group. In contrast, serum ALT, ALP, AST,

and LDH activities in the BBR+MTX- and UMB+MTX-treated animals significantly decreased with respect to the MTX-treated group. So, BBR and UMB protected the liver (hepatocytes) from liver injury (Fig. 1).

Histopathological examination of the liver showed the normal histological structure of hepatic lobule and sinusoids in normal control, BBR, and UMB groups. Histological assessments clearly indicated severe histopathological changes for rats treated with MTX in the form of cytoplasmic vacuolation of hepatocytes, inflammatory cell infiltration (red arrow), and congestion of both central veins and hepatic sinusoids (yellow arrow). Combined administration of MTX with BBR or UMB resulted in obvious improvement of the liver histological architecture with slight vacuolation of some hepatocytes (green arrow) as depicted in Table 2 and Fig. 2.

### Effect of BBR and UMB on hepatic oxidative stress biomarkers

Methotrexate administration resulted in massive production of hepatic oxidative injury as observed by the increase in both MDA and NO<sub>2</sub><sup>-</sup> contents and decrease in both GSH content

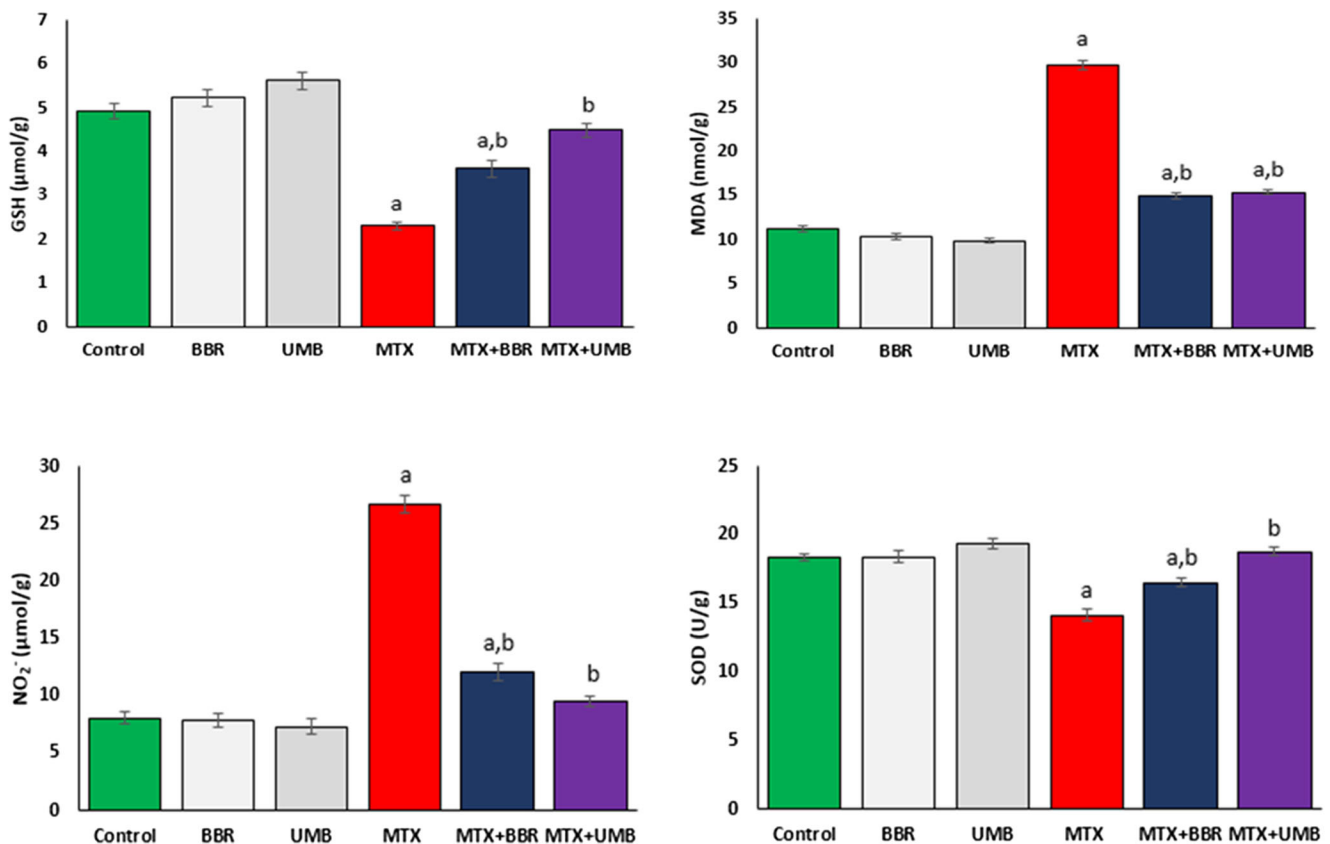


**Fig. 3** Effect of BBR and UMB on hepatic GSH, MDA, and NO<sub>2</sub><sup>-</sup> contents and SOD enzymatic activity. BBR, berberine; UMB, umbelliferone; MTX, methotrexate; GSH, reduced glutathione; MDA, malondialdehyde; NO<sub>2</sub><sup>-</sup>, nitrite; SOD, superoxide dismutase. Data were

presented as mean of 8 rats  $\pm$  SEM. Statistical analysis was performed by using one-way ANOVA followed by Tukey's post hoc comparison test. <sup>a</sup>Statistically significant difference from normal control group at  $P < 0.05$ . <sup>b</sup>Statistically significant difference from MTX group at  $P < 0.05$

and SOD activity with respect to control animals. On the contrary, BBR+MTX or UMB+MTX co-treatment markedly decreased both MDA and NO<sub>2</sub><sup>-</sup> contents, while GSH content and SOD activity were elevated with respect to the rats given MTX only (Fig. 3).

### The impact of BBR and UMB on P<sub>38</sub>MAPK/NF-κB signaling pathway

With regard to the normal control group, the current study demonstrated that the hepatic P<sub>38</sub>MAPK gene was significantly

upregulated in rats given MTX alone. Conversely, co-treatment of BBR or UMB with MTX resulted in a marked downregulation of the P<sub>38</sub>MAPK gene (Fig. 4). Additionally, our data demonstrated that the hepatic NF-κB gene was significantly upregulated in rats given MTX alone, which was attenuated by the administration of BBR and UMB with MTX (Fig. 5).

### Effect of BBR and UMB on Keap-1/Nrf-2 pathway

It was observed that the gene expression of Nrf-2 significantly declined in MTX-intoxicated rats, while the

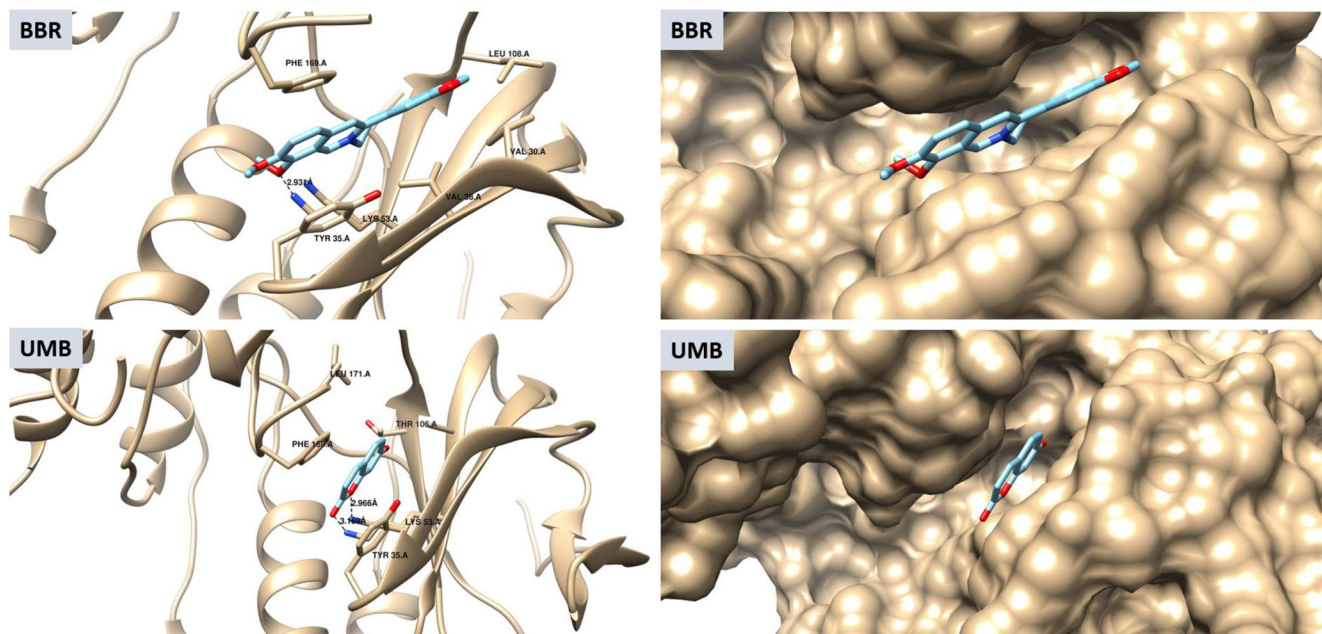
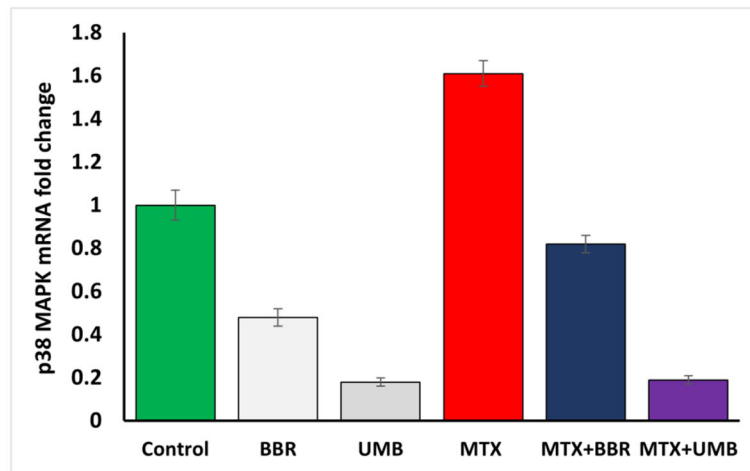


**Fig. 4** Effect of BBR and UMB on hepatic P<sub>38</sub>MAPK expression levels of MTX-treated rats. BBR, berberine; UMB, umbelliferone; MTX, methotrexate; P38MAPK, P<sub>38</sub> mitogen activated protein kinase. Data were presented as mean of 8 rats ± SEM. Statistical analysis was performed by using one-way ANOVA followed by Tukey’s post hoc comparison test. <sup>a</sup>Statistically significant difference from normal control group at *P* < 0.05. <sup>b</sup>Statistically significant difference from MTX group at *P* < 0.05. In

silico evidence for the binding of BBR and UMB to P<sub>38</sub>MAPK protein. BBR forms a hydrogen bond with the side chain of K53, π-π interactions with the aromatic rings of the side chain of Y35 and F169, and hydrophobic interaction with the side chain of V30, V38, and L108. UMB forms two hydrogen bonds with K53 and π-π interactions with the aromatic ring of F169

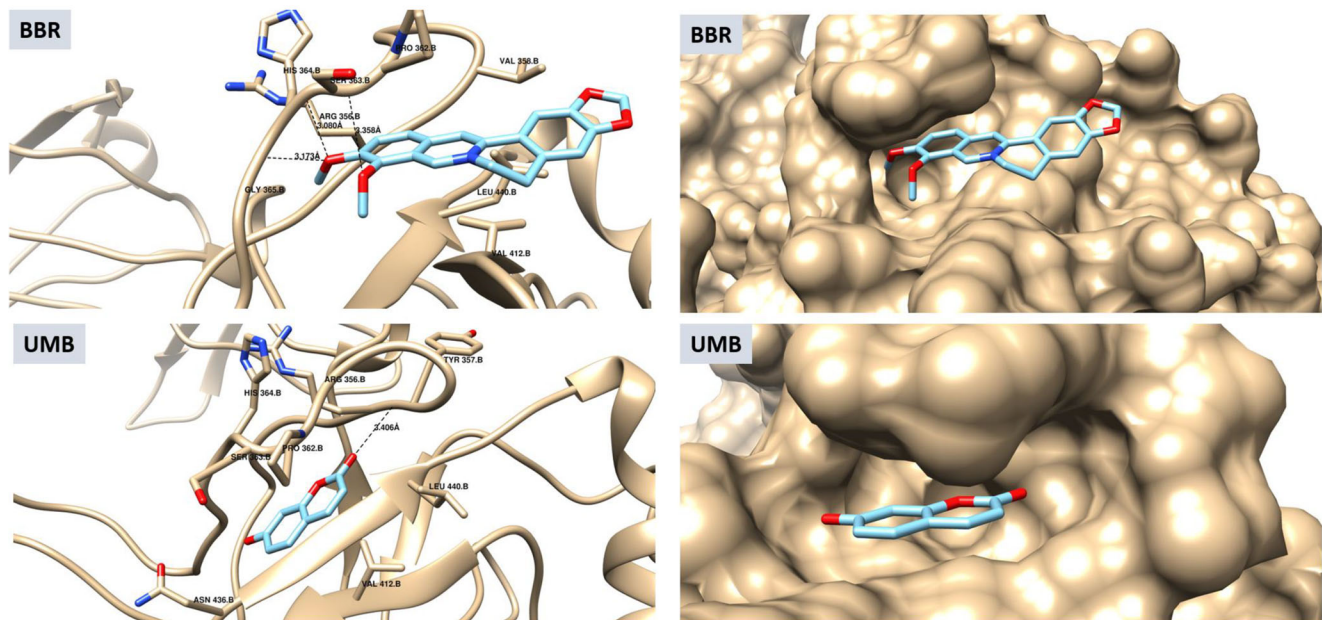
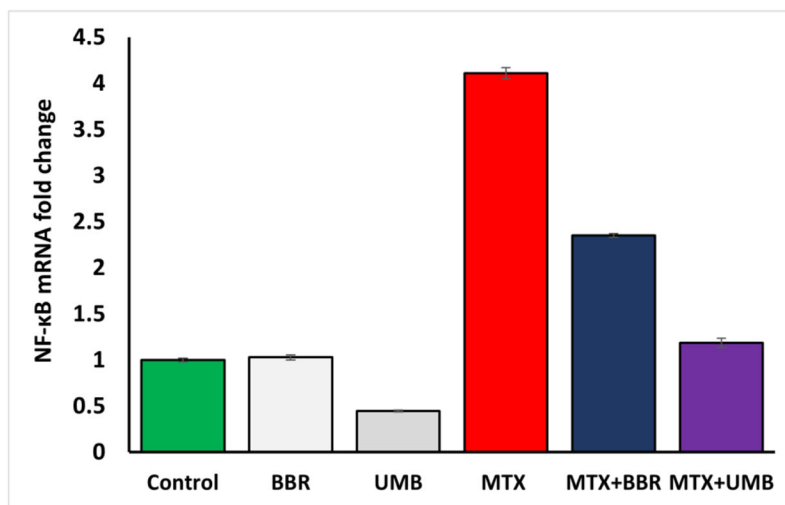


**Fig. 5** Effect of BBR and UMB on hepatic NF- $\kappa$ B expression levels of MTX-treated rats. BBR, berberine; UMB, umbelliferone; MTX, methotrexate; NF- $\kappa$ B, nuclear factor kappa-B. Data were presented as mean of 8 rats  $\pm$  SEM. Statistical analysis was performed by using one-way ANOVA followed by Tukey's post hoc comparison test. <sup>a</sup>Statistically significant difference from normal control group at  $P < 0.05$ . <sup>b</sup>Statistically significant difference from MTX group at  $P < 0.05$ .

In silico evidence for the binding of BBR and UMB to NF- $\kappa$ B protein. BBR forms three hydrogen bonds with S363, H364, and G365. It shows hydrophobic interaction with the side chain of non-polar residues in the active site like V358, V412, and L440, and its aromatic ring exhibits CH/ $\pi$  interaction with the polarized C–H bonds of P362. UMB forms a hydrogen bond with R356 and CH/ $\pi$  interaction with P362.

hepatic Keap-1 gene markedly increased in comparison to that of the normal control. In contrast, the group of rats given BBR+MTX or UMB+MTX showed a remarkable reversal of the aberrant expression of both Nrf-2 and Keap-1 genes in the liver as compared with MTX-treated rats (Fig. 6).

### Effect of BBR and UMB on Bax/Bcl-2/caspase-3 pathway

In our study, Bax, Bcl-2, and caspase-3 hepatic protein expressions were analyzed by immunohistochemistry. The immunohistochemical investigation of Bax, Bcl-2,

and caspase-3 proteins exhibited a strong expression of both hepatic Bax and caspase-3 as well as a weak expression of Bcl-2 of MTX-treated rats when compared with the expression of normal rats. Meanwhile, these changes were strongly modulated by BBR and UMB treatment as evidenced by weak expression of both Bax and caspase-3 along with strong expression of Bcl-2 (Figs. 7, 8, and 9).

### In silico evidence

A molecular docking approach has been used to predict the binding affinity of BBR and UMB against Keap-1,



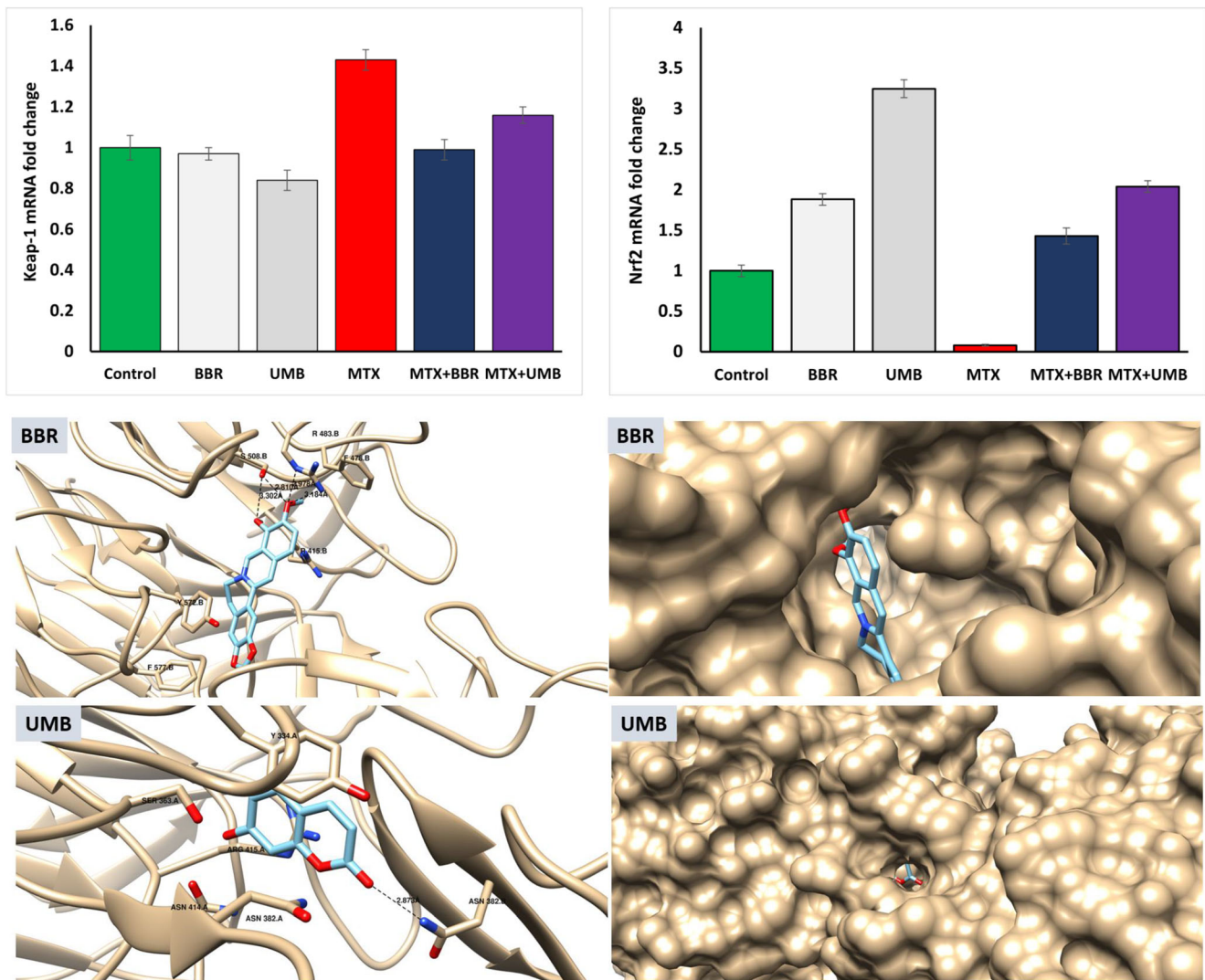


**Fig. 6** Effect of BBR and UMB on hepatic Nrf-2 and Keap-1 mRNA expression levels of MTX-treated rats. BBR, berberine; UMB, umbelliferone; MTX, methotrexate; Nrf-2, nuclear factor erythroid 2-related factor-2; and Keap-1, Kelch-like ECH-associated protein-1. Data were presented as mean of 8 rats ± SEM. Statistical analysis was performed by using one-way ANOVA followed by Tukey’s post hoc comparison test. <sup>a</sup>Statistically significant difference from normal control

group at  $P < 0.05$ .<sup>b</sup>Statistically significant difference from MTX group at  $P < 0.05$ . In silico evidence for the binding of BBR and UMB to Keap-1 protein. BBR forms four hydrogen bonds with the side chain of R483 and S508 and  $\pi$ - $\pi$  interactions with the aromatic ring of the side chain of Y572. UMB forms a hydrogen bond with the side chain of N382 and  $\pi$ - $\pi$  interactions with the aromatic ring Y334

$P_{38}$ MAPK, and NF- $\kappa$ B. The unique tetracyclic skeleton and multiple polar groups of BBR encourage both the hydrophobic and electrostatic interaction with the target proteins. BBR exhibited high binding affinity to Keap-1,  $P_{38}$ MAPK, and NF- $\kappa$ B with docking energy  $-8.96 \pm 0.23$  kcal/mol,  $-9.44 \pm 0.60$  kcal/mol, and  $-7.50 \pm 0.47$  kcal/mol, respectively. For  $P_{38}$ MAPK, BBR forms a hydrogen bond with the side chain of K53,  $\pi$ - $\pi$  interactions with the aromatic rings of the side chain of Y35 and F169, and hydrophobic interaction with the side chain of V30, V38, and L108 (Fig. 4). For NF- $\kappa$ B, BBR forms three hydrogen bonds with S363, H364, and G365. It shows hydrophobic interaction with the side chain of non-polar residues in the active site like V358, V412, and L440,

and its aromatic ring exhibits CH/ $\pi$  interaction with the polarized C–H bonds of P362 (Fig. 5). For Keap-1, BBR forms four hydrogen bonds with the side chain of R483 and S508 and  $\pi$ - $\pi$  interactions with the aromatic ring of the side chain of Y572 (Fig. 6). These non-covalent interactions promote the fitting of BBR in the binding pocket as illustrated in the surface map of proteins.

Umbelliferone is a 7-hydroxycoumarin that showed a promising binding affinity to Keap-1,  $P_{38}$ MAPK, and NF- $\kappa$ B with docking energy  $-6.43 \pm 0.22$  kcal/mol,  $-6.85 \pm 0.56$  kcal/mol, and  $-6.13 \pm 0.16$  kcal/mol, respectively. For  $P_{38}$ MAPK, UMB forms two hydrogen bonds with K53 and  $\pi$ - $\pi$  interactions with the aromatic ring of F169 (Fig. 4). For

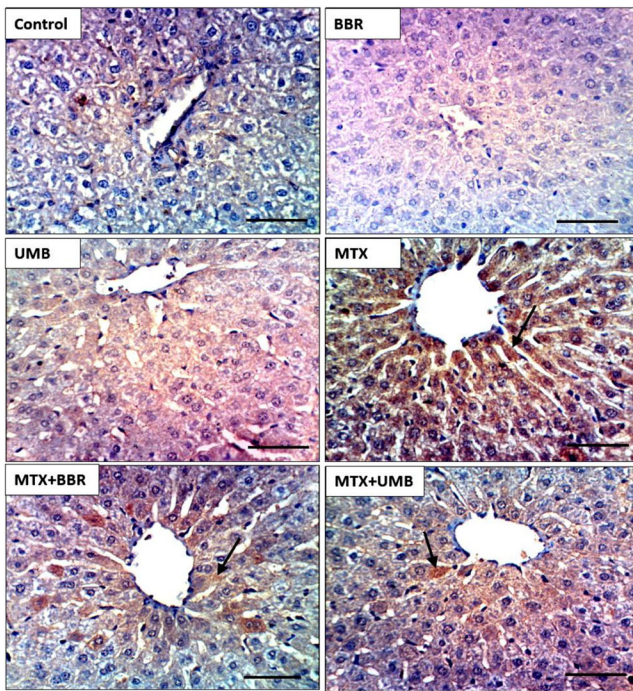
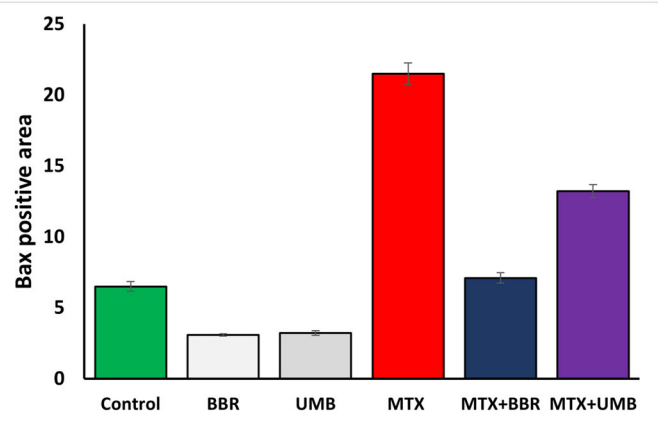


**Fig. 7** Effect of BBR and UMB on hepatic Bax protein expression level of MTX-treated rats. BBR, berberine; UMB, umbelliferone; MTX, methotrexate; Bax, Bcl-2-associated X protein. Data were presented as mean of 8 rats  $\pm$  SEM. Statistical analysis was performed by using one-way



ANOVA followed by Tukey's post hoc comparison test. <sup>a</sup>Statistically significant difference from normal control group at  $P < 0.05$ . <sup>b</sup>Statistically significant difference from MTX group at  $P < 0.05$

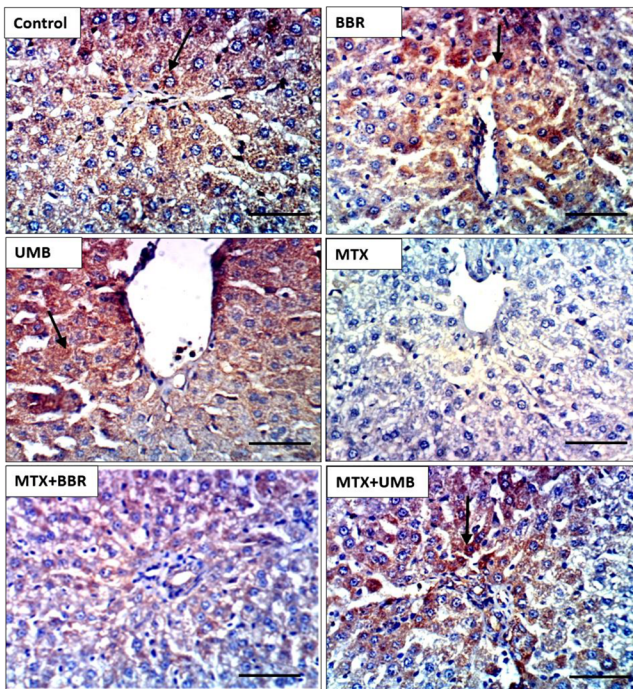
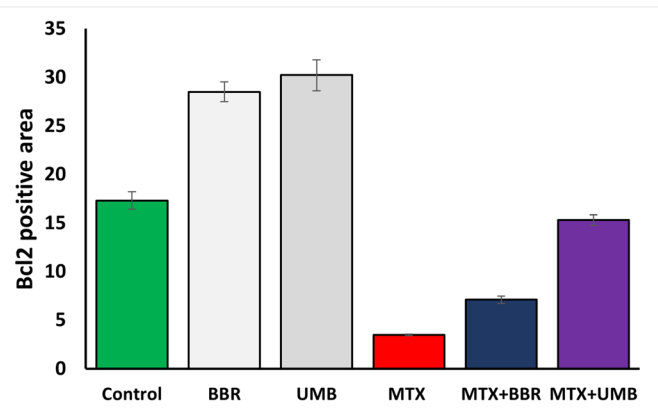


**Fig. 8** Effect of BBR and UMB on hepatic Bcl-2 protein expression level of MTX-treated rats. BBR, berberine; UMB, umbelliferone; MTX, methotrexate; Bcl-2, B-cell lymphoma 2. Data were presented as mean of 8 rats  $\pm$  SEM. Statistical analysis was performed by using one-way



ANOVA followed by Tukey's post hoc comparison test. <sup>a</sup>Statistically significant difference from normal control group at  $P < 0.05$ . <sup>b</sup>Statistically significant difference from MTX group at  $P < 0.05$

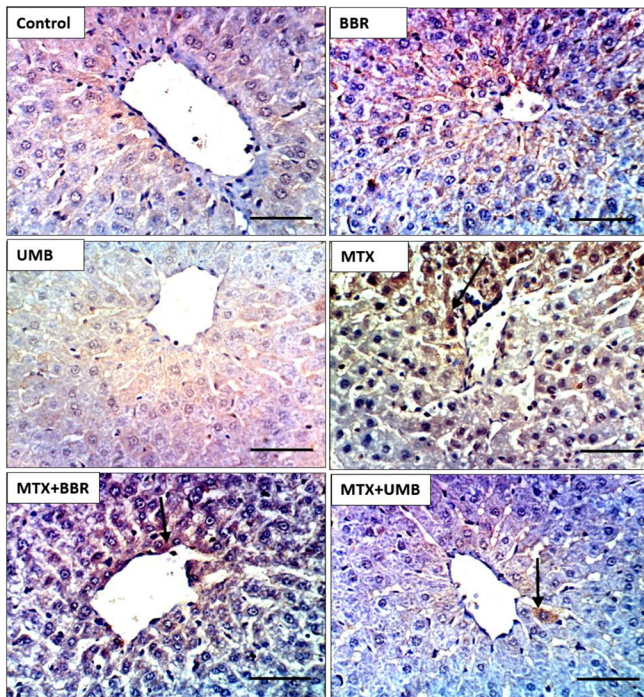
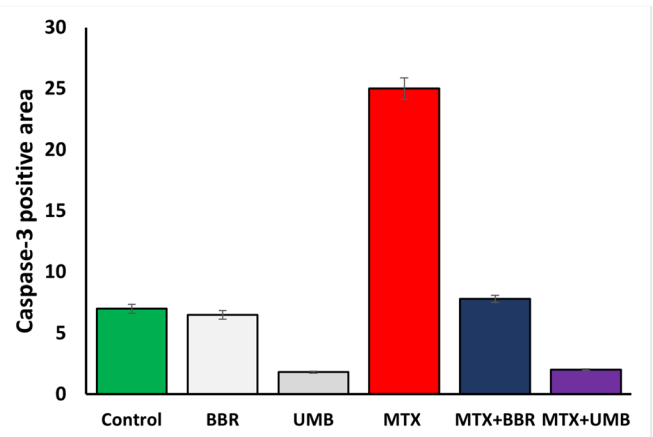


**Fig. 9** Effect of BBR and UMB on hepatic caspase-3 protein expression level of MTX-treated rats. BBR, berberine; UMB, umbelliferone; MTX, methotrexate. Data were presented as mean of 8 rats ± SEM. Statistical analysis was performed by using one-way ANOVA followed by Tukey’s



post hoc comparison test. <sup>a</sup>Statistically significant difference from normal control group at  $P < 0.05$ . <sup>b</sup>Statistically significant difference from MTX group at  $P < 0.05$

NF- $\kappa$ B, UMB forms a hydrogen bond with R356 and CH/ $\pi$  interaction with P362 (Fig. 5). For Keap-1, UMB forms a hydrogen bond with the side chain of N382 and  $\pi$ - $\pi$  interactions with the aromatic ring Y334 (Fig. 6). UMB showed a well-fitted structure in the active site of the proteins, as shown in the surface map of the docked structures.

## Discussion

Intriguingly, toxicities associated with classical chemotherapeutic drugs have a significant impact on the outcome of patients receiving chemotherapy. These adverse effects often limit their efficiency. Since the liver detoxifies the xenobiotics in the body, it is regarded as the first target organ that encounters all toxic drugs and chemicals. Notably, toxicities associated with MTX are dose dependent (Howard et al. 2016). Accordingly, a large area of research interest focused on adjuvant therapies for patients with cancer in order to get a better response with lower toxicities. Accumulated evidence demonstrated that increasing the generation of ROS plays a key role in MTX-induced hepatic intoxication. ROS formations release pro-inflammatory cytokines that induce apoptosis and hepatocytes damage (Abdel-Wahab et al. 2020; Khalifa et al. 2017).

Compounds of natural origin have received great interest; these compounds can provide relative protection against

oxidative stress injury. These natural products are an available source of effective and alternative treatment for liver disorders. Antioxidants are agents that protect against oxidative cell injury through electron donation and neutralization of free radicals (Saeidnia and Abdollahi 2013; Sayed et al. 2020). However, there is little knowledge on the molecular mechanisms of these products and their biological properties. Therefore, the aim of the current study is to investigate the underlying molecular mechanisms involved in the hepatoprotection of BBR and UMB on MTX-induced hepatic injury for more clarification and full understanding leading to move a step towards the translational application of BBR and UMB in cancer protocols.

We provided the first evidence that co-administration of BBR or UMB with MTX remarkably attenuated MTX hepatotoxicity in rats, as demonstrated by the reduction in ALT, ALP, AST, and LDH activities and inflammatory cell infiltration into the liver. It is attributed to the alteration of the membrane permeability due to the hepatic injury that leads to a leakage of these enzymes.

Mitigating oxidative stress and boosting antioxidant defense mechanisms mediate the protective effect of BBR or UMB against hepatic injury. In the present investigation, hepatic MDA and  $\text{NO}_2^-$  contents were significantly enhanced by MTX, whereas the content of GSH and the activity of SOD were remarkably suppressed in the MTX-treated group. These results agree with previous studies done by Fayez et al. (2018)

and Bu et al. (2018). It has been noted that lipid peroxidation resulted from MTX caused mitochondrial dysfunction (Tabassum et al. 2010). BBR or UMB co-treatment with MTX dramatically recovered these disordered changes in the liver due to the antioxidant ability of BBR. Li et al. (2014) reported that BBR antioxidant capacity is due to its direct free radical scavenging, increased SOD expression, and NADPH oxidase inhibition. Also, some studies mentioned that UMB had shown antioxidant efficacy in different hepatotoxicity models, including carbon tetrachloride (Mahmoud et al. 2019a) and N-nitrosodiethylamine (Subramaniam and Ellis 2016).

An increasing body of evidence reported that liver injury is related to the increased generation of inflammatory mediators caused by leukocyte invasion into the site of injury. Furthermore, reports have shown that ROS increases the expression of inflammatory mediators and NF- $\kappa$ B (Jaeschke 2011). The most important pathway through which ROS exert an effect on gene transcription is via NF- $\kappa$ B (Gloire et al. 2006; Morgan and Liu 2011). P<sub>38</sub>MAPK pathway positively regulates NF- $\kappa$ B, which is regarded as an important controller

of the inflammatory response (Cuadrado and Nebreda 2010). The NF- $\kappa$ B pathway is one of the best-known pathways that are involved in the pathogenesis of different illnesses (Robinson and Mann 2010). In the present study, MTX-BBR co-treatment remarkably decreased the expression levels of P<sub>38</sub>MAPK as well as NF- $\kappa$ B in the liver of rats, indicating that P<sub>38</sub>MAPK/NF- $\kappa$ B pathway is implicated in MTX hepatotoxicity. This finding clearly supports the notion that BBR could inhibit the inflammatory response via its ability to downregulate P<sub>38</sub>MAPK/NF- $\kappa$ B expression.

Importantly, Nrf-2 is a strategic controller of the antioxidant process, as it regulates several detoxifying genes responsible for combating oxidative stress. Therefore, the Keap-1/Nrf-2 system has a vital role in regulating cell homeostasis (Deshmukh et al. 2017; Ma 2013). Wu et al. (2011) reported that activation of Nrf-2 by hepatocyte-specific Keap-1 knock-out in mice leads to an increase in the hepatic concentration of NADPH and resulted in the protection of the liver from ROS (Wu et al. 2011). Additionally, strong evidence has indicated that ROS generation stimulates cytokine releases such as iNOS and COX-2 (Ali et al. 2017). Our study demonstrated

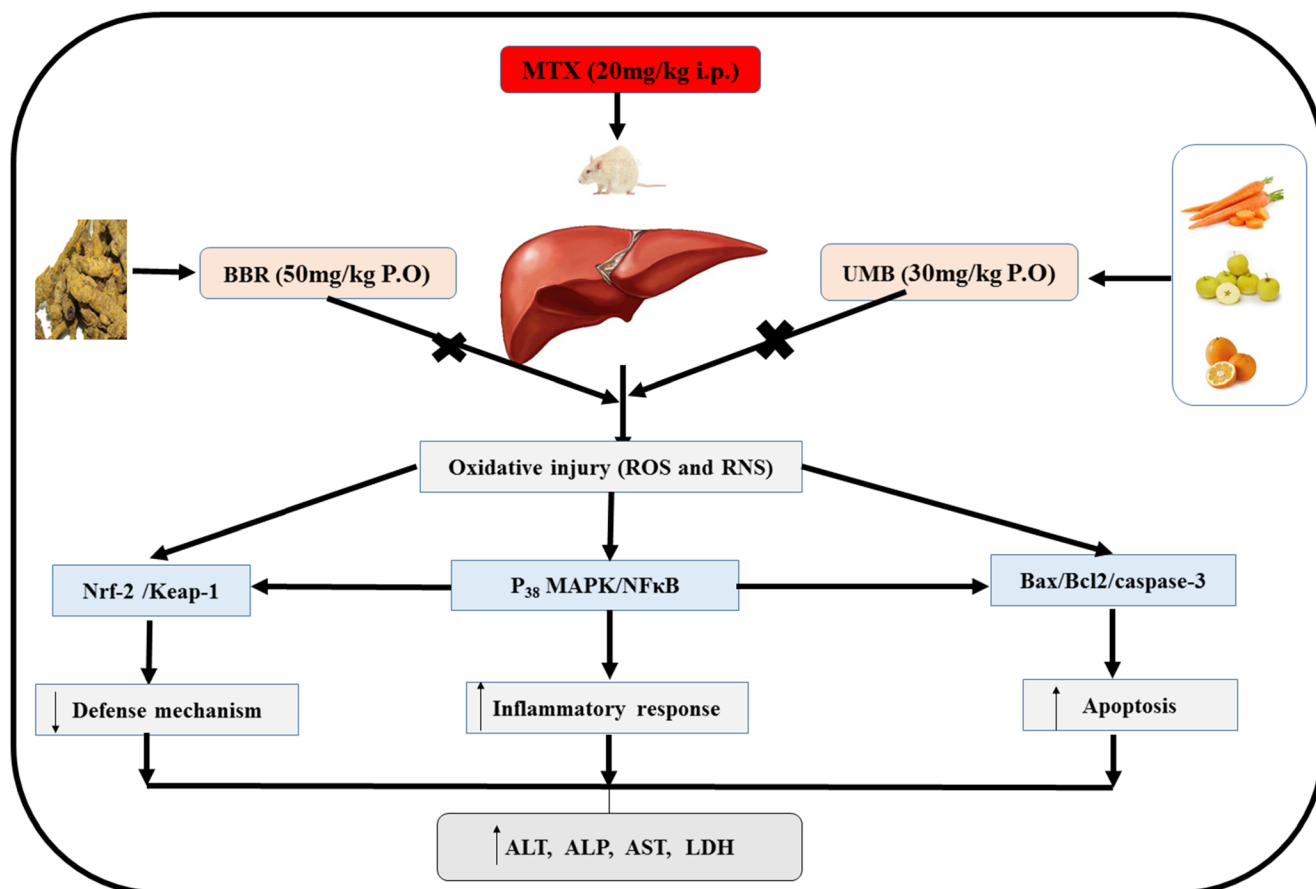


**Fig. 10** Proposed mechanisms for hepatoprotective effects of BBR and UMB against MTX-induced hepatic intoxication. BBR, berberine; UMB, umbelliferone; MTX, methotrexate; ALT, alanine aminotransferase; ALP, alkaline phosphatase; AST, aspartate aminotransferase; LDH, lactate dehydrogenase; ROS, reactive oxygen species; ROS, reactive

nitrogen species; P<sub>38</sub>MAPK, P<sub>38</sub> mitogen-activated protein kinase; NF- $\kappa$ B, nuclear factor kappa-B; Keap-1, Kelch-like ECH-associated protein 1; Nrf-2, nuclear factor erythroid 2-related factor2; Bax, Bcl-2 associated X protein; and Bcl-2, B-cell lymphoma 2

that BBR and UMB significantly attenuated the lipid peroxidation level and inflammatory response, followed by activation of Nrf-2 nuclear translocation in the hepatic tissues. Hence, the results of this study suggested that co-administration of BBR or UMB with MTX protects against MTX-induced oxidative liver injury through the activation of Nrf-2. Accumulated Nrf-2 activates antioxidant and cytoprotective enzymes, and subsequently, BBR and UMB may inhibit inflammation and oxidative damage.

Then, we aimed to explore the modulatory effect of BBR and UMB on Keap-1, P<sub>38</sub>MAPK, and NF- $\kappa$ B. Therefore, molecular docking was done to examine their binding modes. The structural features of BBR and UMB allowed them to form different non-covalent interactions with the active sites of Keap-1, P<sub>38</sub>MAPK, and NF- $\kappa$ B. BBR showed a higher binding affinity with the target proteins as compared to UMB. However, both drugs produced a promising inhibition of Keap1, P<sub>38</sub>MAPK, and NF- $\kappa$ B. The findings of the docking studies support our hypothesis and emphasize the antioxidant and anti-inflammatory role of BBR and UMB as protective agents against hepatic injury.

Finally, oxidative injury together with the inflammatory response induces hepatic apoptosis (Jaeschke 2011). Interestingly, one of the important and major strategic regulators of the apoptosis process is Bcl-2 family proteins (Chao and Korsmeyer 1998). Bax may bind to Bcl-2, forming Bax/Bcl-2 heterodimers. The ratio of Bax to Bcl-2 determines the susceptibility of a cell to apoptosis (Khodapasand et al. 2015). Here, MTX-induced rats markedly upregulated both Bax and caspase-3 proteins, while the level of anti-apoptotic protein Bcl-2 significantly decreased. These findings might be explained in terms of the MTX-induced inflammation and oxidative stress in the liver of rats. Co-administration of BBR or UMB with MTX markedly prevented MTX-induced apoptosis through downregulation of both Bax and caspase-3 proteins along with upregulation of Bcl-2 protein. It may be attributed to its capability to attenuate ROS. In line with this, Eissa et al. (2018) reported a decrease in both Bax and caspase-3 protein expressions in the liver fibrosis rat model induced by thioacetamide following treatment with BBR.

## Conclusion

Collectively, the current results confirmed the hepatoprotection of BBR and UMB against hepatic intoxication induced by MTX. BBR and UMB have potent antioxidant, anti-inflammatory, and anti-apoptotic activities. Our data clarified the underlying molecular mechanism of hepatoprotective effects of BBR and UMB as indicated by well regulation of Keap-1/Nrf-2 and P<sub>38</sub>MAPK/NF- $\kappa$ B and Bax/Bcl-2/

caspase-3 signaling pathways. In addition, our obtained data indicated a close relationship between these signaling pathways (Fig. 10).

**Abbreviations** BBR, Berberine; UMB, Umbelliferone; MTX, Methotrexate; ALT, Alanine aminotransferase; ALP, Alkaline phosphatase; AST, Aspartate aminotransferase; LDH, Lactate dehydrogenase; ROS, Reactive oxygen species; MDA, Malondialdehyde; NO<sub>2</sub>, Nitrite; GSH, Reduced glutathione; SOD, Superoxide dismutase; P<sub>38</sub>MAPK, P<sub>38</sub> mitogen-activated protein kinase; NF- $\kappa$ B, Nuclear factor kappa-B cells; Keap-1, Kelch-like ECH-associated protein 1; Nrf-2, Nuclear factor erythroid 2-related factor 2; qRT-PCR, Quantitative real-time polymerase chain reaction; IHC, Immunohistochemistry; Bax, Bcl-2-associated X protein; Bcl-2, B-cell lymphoma 2

**Acknowledgements** We would like to thank Dr. Kawkab A. Ahmed, Professor of Pathology, Faculty of Veterinary Medicine, Cairo University, Egypt, for her kind help in histopathology and immunohistochemistry.

**Author contribution** RAMH, AMS, MMK, ASS, and EHMH shared in the conception, experiments, and interpretation of the results. WRM and EMHM analyzed data. WRM, ASS, AMS, and MMK shared in writing the manuscript. The final version of the manuscript has been approved by all authors.

**Data availability** The datasets used and/or analyzed during the current study are available from the corresponding author on reasonable request.

## Declarations

**Ethics approval and consent to participate** All animal handling and experiment procedures were approved by the ethical committee in Assiut University, Egypt (License no: 17200074).

**Consent for publication** Not applicable.

**Competing interests** The authors declare no competing interests.

## References

- Abdel-Wahab BA, Ali FEM, Alkahtani SA, Alshabi AM, Mahnashi MH, Hassanein EHM (2020) Hepatoprotective effect of rebamipide against methotrexate-induced hepatic intoxication: role of Nrf2/GSK-3 $\beta$ , NF- $\kappa$ B-p65/JAK1/STAT3, and PUMA/Bax/Bcl-2 signaling pathways. *Immunopharmacol Immunotoxicol* 42(5): 493–503. <https://doi.org/10.1080/08923973.2020.1811307>
- Akanda MR, Kim IS, Ahn D, Tae HJ, Tian W, Nam HH, Choo BK, Park BY (2017) In vivo and in vitro hepatoprotective effects of Geranium koreanum methanolic extract via downregulation of MAPK/caspase-3 pathway. *Evid Based Complement Alternat Med* 2017: 8137627–8137612. <https://doi.org/10.1155/2017/8137627>
- Ali N, Rashid S, Nafees S, Hasan SK, Shahid A, Majed F, Sultana S (2017) Protective effect of chlorogenic acid against methotrexate induced oxidative stress, inflammation and apoptosis in rat liver: an experimental approach. *Chem Biol Interact* 272:80–91. <https://doi.org/10.1016/j.cbi.2017.05.002>
- Ali FEM, Hassanein EHM, Bakr AG, El-Shoura EAM, El-Gamal DA, Mahmoud AR, Abd-Elhamid TH (2020) Ursodeoxycholic acid abrogates gentamicin-induced hepatotoxicity in rats: role of NF- $\kappa$ B-

- p65/TNF- $\alpha$ , Bax/Bcl-xl/caspase-3, and eNOS/iNOS pathways. *Life Sci* 254:117760. <https://doi.org/10.1016/j.lfs.2020.117760>
- Almani SA, Memon IA, Shaikh TZ, Khoharo HK, Ujjan I (2017) Berberine protects against metformin-associated lactic acidosis in induced diabetes mellitus. *Iran J Basic Med Sci* 20:511–515. <https://doi.org/10.22038/ijbms.2017.8675>
- Alotaibi MF, Al-Joufi F, Abou Seif HS, Alzoghbaibi MA, Djouhri L, Ahmeda AF, Mahmoud AM (2020) Umbelliferone inhibits spermatogenic defects and testicular injury in lead-intoxicated rats by suppressing oxidative stress and inflammation, and improving Nrf2/HO-1 signaling. *Drug Des Dev Ther* 14:4003–4019. <https://doi.org/10.2147/dddt.S265636>
- Azevedo R, van Zeeland M, Raaijmakers H, Kazemier B, de Vlieg J, Oubrie A (2012) X-ray structure of p38 $\alpha$  bound to TAK-715: comparison with three classic inhibitors. *Acta Crystallogr D Biol Crystallogr* 68:1041–1050. <https://doi.org/10.1107/S090744491201997x>
- Bancroft JD, Gamble M (2008) Theory and practice of histological techniques. Elsevier health sciences
- Bataille AM, Manautou JE (2012) Nrf2: a potential target for new therapeutics in liver disease. *Clin Pharmacol Ther* 92:340–348. <https://doi.org/10.1038/clpt.2012.110>
- Belfield A, Goldberg DM (1971) Normal ranges and diagnostic value of serum 5' nucleotidase and alkaline phosphatase activities in infancy. *Arch Dis Child* 46:842–846. <https://doi.org/10.1136/adc.46.250.842>
- Brown PM, Pratt AG, Isaacs JD (2016) Mechanism of action of methotrexate in rheumatoid arthritis, and the search for biomarkers. *Nat Rev Rheumatol* 12:731–742. <https://doi.org/10.1038/nrrheum.2016.175>
- Bu T, Wang C, Meng Q, Huo X, Sun H, Sun P, Zheng S, Ma X, Liu Z, Liu K (2018) Hepatoprotective effect of rhein against methotrexate-induced liver toxicity. *Eur J Pharmacol* 834:266–273. <https://doi.org/10.1016/j.ejphar.2018.07.031>
- Chao DT, Korsmeyer SJ (1998) BCL-2 family: regulators of cell death. *Annu Rev Immunol* 16:395–419. <https://doi.org/10.1146/annurev.immunol.16.1.395>
- Chen FE, Huang DB, Chen YQ, Ghosh G (1998) Crystal structure of p50/p65 heterodimer of transcription factor NF-kappaB bound to DNA. *Nature* 391:410–413. <https://doi.org/10.1038/34956>
- Chu X, Wang H, Jiang YM, Zhang YY, Bao YF, Zhang X, Zhang JP, Guo H, Yang F, Luan YC, Dong YS (2016) Ameliorative effects of tannic acid on carbon tetrachloride-induced liver fibrosis in vivo and in vitro. *J Pharmacol Sci* 130:15–23. <https://doi.org/10.1016/j.jphs.2015.12.002>
- Cuadrado A, Nebreda AR (2010) Mechanisms and functions of p38 MAPK signalling. *Biochem J* 429:403–417. <https://doi.org/10.1042/bj20100323>
- Deshmukh P, Unni S, Krishnappa G, Padmanabhan B (2017) The Keap1-Nrf2 pathway: promising therapeutic target to counteract ROS-mediated damage in cancers and neurodegenerative diseases. *Biophys Rev* 9:41–56. <https://doi.org/10.1007/s12551-016-0244-4>
- Eissa LA, Kenawy HI, El-Karef A, Elsherbiny NM, El-Mihi KA (2018) Antioxidant and anti-inflammatory activities of berberine attenuate hepatic fibrosis induced by thioacetamide injection in rats. *Chem Biol Interact* 294:91–100. <https://doi.org/10.1016/j.cbi.2018.08.016>
- Ellman GL (1959) Tissue sulfhydryl groups. *Arch Biochem Biophys* 82:70–77. [https://doi.org/10.1016/0003-9861\(59\)90090-6](https://doi.org/10.1016/0003-9861(59)90090-6)
- Fayez AM, Zakaria S, Moustafa D (2018) Alpha lipoic acid exerts anti-oxidant effect via Nrf2/HO-1 pathway activation and suppresses hepatic stellate cells activation induced by methotrexate in rats. *Biomed Pharmacother* 105:428–433. <https://doi.org/10.1016/j.biopha.2018.05.145>
- Germoush MO, Othman SI, al-Qaraawi MA, al-Harbi HM, Hussein OE, al-Basher G, Alotaibi MF, Elgebaly HA, Sandhu MA, Allam AA, Mahmoud AM (2018) Umbelliferone prevents oxidative stress, inflammation and hematological alterations, and modulates glutamate-nitric oxide-cGMP signaling in hyperammonemic rats. *Biomed Pharmacother* 102:392–402. <https://doi.org/10.1016/j.biopha.2018.03.104>
- Gloire G, Legrand-Poels S, Piette J (2006) NF-kappaB activation by reactive oxygen species: fifteen years later. *Biochem Pharmacol* 72:1493–1505. <https://doi.org/10.1016/j.bcp.2006.04.011>
- Hassanein EHM, Sayed AM, Hussein OE, Mahmoud AM (2020) Coumarins as modulators of the Keap1/Nrf2/ARE signaling pathway. *Oxidative Med Cell Longev* 2020:1675957–1675925. <https://doi.org/10.1155/2020/1675957>
- Hassanein EHM, Ali FEM, Kozman MR, Abd El-Ghaffar OAM (2021) Umbelliferone attenuates gentamicin-induced renal toxicity by suppression of TLR-4/NF- $\kappa$ B-p65/NLRP-3 and JAK1/STAT-3 signaling pathways. *Environ Sci Pollut Res Int* 28(9):11558–11571. <https://doi.org/10.1007/s11356-020-11416-5>
- Herman S, Zurgil N, Deutsch M (2005) Low dose methotrexate induces apoptosis with reactive oxygen species involvement in T lymphocytic cell lines to a greater extent than in monocytic lines. *Inflamm Res* 54:273–280. <https://doi.org/10.1007/s00011-005-1355-8>
- Hosseini H, Teimouri M, Shabani M, Koushki M, Babaei Khorzoughi R, Namvarjah F, Izadi P, Meshkani R (2020) Resveratrol alleviates non-alcoholic fatty liver disease through epigenetic modification of the Nrf2 signaling pathway. *Int J Biochem Cell Biol* 119:105667. <https://doi.org/10.1016/j.biocel.2019.105667>
- Howard SC, McCormick J, Pui CH, Buddington RK, Harvey RD (2016) Preventing and managing toxicities of high-dose methotrexate. *Oncologist* 21:1471–1482. <https://doi.org/10.1634/theoncologist.2015-0164>
- Imenshahidi M, Hosseinzadeh H (2019) Berberine and barberry (*Berberis vulgaris*): a clinical review. *Phytother Res* 33(3):504–523. <https://doi.org/10.1002/ptr.6252>
- Izquierdo JM, Sotorrio P, Alvarez-Uria J, Estrada JM, Quirós A (1982) Serum ASAT, ALAT, ALP, LD, GT, and CK determined in the Cobas-Bio centrifugal analyser by the methods of the Scandinavian Committee on Enzymes. *Scand J Clin Lab Invest* 42:173–176. <https://doi.org/10.1080/00365518209168069>
- Jaeschke H (2011) Reactive oxygen and mechanisms of inflammatory liver injury: present concepts. *J Gastroenterol Hepatol* 26(Suppl 1):173–179. <https://doi.org/10.1111/j.1440-1746.2010.06592>
- Jnoff E, Albrecht C, Barker JJ, Barker O, Beaumont E, Bromidge S, Brookfield F, Brooks M, Bubert C, Ceska T, Corden V, Dawson G, Duclos S, Fryatt T, Genicot C, Jigorel E, Kwong J, Maghames R, Mushi I, Pike R, Sands ZA, Smith MA, Stimson CC, Courade JP (2014) Binding mode and structure-activity relationships around direct inhibitors of the Nrf2-Keap1 complex. *Chem Med Chem* 9:699–705. <https://doi.org/10.1002/cmdc.201300525>
- Kamel EO, Hassanein EHM, Ahmed MA, Ali FEM (2020) Perindopril ameliorates hepatic ischemia reperfusion injury via regulation of NF- $\kappa$ B-p65/TLR-4, JAK1/STAT-3, Nrf-2, and PI3K/Akt/mTOR signaling pathways. *Anat Rec (Hoboken)* 303:1935–1949. <https://doi.org/10.1002/ar.24292>
- Khalifa MMA, Bakr AG, Osman AT (2017) Protective effects of phloridzin against methotrexate-induced liver toxicity in rats. *Biomed Pharmacother* 95:529–535. <https://doi.org/10.1016/j.biopha.2017.08.121>
- Khodapasand E, Jafarzadeh N, Farrokhi F, Kamalidehghan B, Houshmand M (2015) Is Bax/Bcl-2 ratio considered as a prognostic marker with age and tumor location in colorectal cancer? *Iran Biomed J* 19:69–75. <https://doi.org/10.6091/ibj.1366.2015>
- Li Z, Geng YN, Jiang JD, Kong WJ (2014) Antioxidant and anti-inflammatory activities of berberine in the treatment of diabetes mellitus. *Evid Based Complement Alternat Med* 2014:289264–289212. <https://doi.org/10.1155/2014/289264>
- Livak KJ, Schmittgen TD (2001) Analysis of relative gene expression data using real-time quantitative PCR and the 2(-Delta Delta C(T))

- method. *Methods* 25:402–408. <https://doi.org/10.1006/meth.2001.1262>
- Luedde T, Schwabe RF (2011) NF- $\kappa$ B in the liver—linking injury, fibrosis and hepatocellular carcinoma. *Nat Rev Gastroenterol Hepatol* 8: 108–118. <https://doi.org/10.1038/nrgastro.2010.213>
- Lv H, Xiao Q, Zhou J, Feng H, Liu G, Ci X (2018) Licochalcone A upregulates Nrf2 antioxidant pathway and thereby alleviates acetaminophen-induced hepatotoxicity. *Front Pharmacol* 9:147. <https://doi.org/10.3389/fphar.2018.00147>
- Ma Q (2013) Role of nrf2 in oxidative stress and toxicity. *Annu Rev Pharmacol Toxicol* 53:401–426. <https://doi.org/10.1146/annurev-pharmtox-011112-140320>
- Mahmoud AM, Hozayen WG, Hasan IH, Shaban E, Bin-Jumah M (2019a) Umbelliferone ameliorates CCl<sub>4</sub>-induced liver fibrosis in rats by upregulating PPAR $\gamma$  and attenuating oxidative stress, inflammation, and TGF- $\beta$ 1/Smad3 signaling. *Inflammation* 42: 1103–1116. <https://doi.org/10.1007/s10753-019-00973-8>
- Mahmoud AR, Ali FEM, Abd-Elhamid TH, Hassanein EHM (2019b) Coenzyme Q(10) protects hepatocytes from ischemia reperfusion-induced apoptosis and oxidative stress via regulation of Bax/Bcl-2/PUMA and Nrf-2/FOXO-3/Sirt-1 signaling pathways. *Tissue Cell* 60:1–13. <https://doi.org/10.1016/j.tice.2019.07.007>
- Malaviya AN (2016) Landmark papers on the discovery of methotrexate for the treatment of rheumatoid arthritis and other systemic inflammatory rheumatic diseases: a fascinating story. *Int J Rheum Dis* 19: 844–851. <https://doi.org/10.1111/1756-185x.12862>
- Marklund S, Marklund G (1974) Involvement of the superoxide anion radical in the autoxidation of pyrogallol and a convenient assay for superoxide dismutase. *Eur J Biochem* 47:469–474. <https://doi.org/10.1111/j.1432-1033.1974.tb03714.x>
- Derelanko MJ (2008) *The Toxicologist's Pocket Handbook* (2nd ed.). CRC Press. <https://doi.org/10.3109/9781420051391>
- Mihara M, Uchiyama M (1978) Determination of malonaldehyde precursor in tissues by thiobarbituric acid test. *Anal Biochem* 86:271–278. [https://doi.org/10.1016/0003-2697\(78\)90342-1](https://doi.org/10.1016/0003-2697(78)90342-1)
- Montgomery H, Dymock JFJA (1961) Determination of nitrite in water. *Analyst* 86(102):414
- Morgan MJ, Liu ZG (2011) Crosstalk of reactive oxygen species and NF- $\kappa$ B signaling. *Cell Res* 21:103–115. <https://doi.org/10.1038/cr.2010.178>
- Muriel P, Gordillo KR (2016) Role of oxidative Stress in liver health and disease. *Oxidative Med Cell Longev* 2016:9037051–9037052. <https://doi.org/10.1155/2016/9037051>
- Newman DJ, Cragg GM (2016) Natural products as sources of new drugs from 1981 to 2014. *J Nat Prod* 79:629–661. <https://doi.org/10.1021/acs.jnatprod.5b01055>
- Nobili S, Lippi D, Witort E, Donnini M, Bausi L, Mini E, Capaccioli S (2009) Natural compounds for cancer treatment and prevention. *Pharmacol Res* 59:365–378. <https://doi.org/10.1016/j.phrs.2009.01.017>
- Porter AG, Jänicke RU (1999) Emerging roles of caspase-3 in apoptosis. *Cell Death Differ* 6:99–104. <https://doi.org/10.1038/sj.cdd.4400476>
- Ramos-Vara JA, Miller MA (2014) When tissue antigens and antibodies get along: revisiting the technical aspects of immunohistochemistry—the red, brown, and blue technique. *Vet Pathol* 51:42–87. <https://doi.org/10.1177/0300985813505879>
- Reitman S, Frankel S (1957) A colorimetric method for the determination of serum glutamic oxalacetic and glutamic pyruvic transaminases. *Am J Clin Pathol* 28:56–63. <https://doi.org/10.1093/ajcp/28.1.56>
- Robinson SM, Mann DA (2010) Role of nuclear factor kappaB in liver health and disease. *Clin Sci (Lond)* 118:691–705. <https://doi.org/10.1042/cs20090549>
- Saeidnia S, Abdollahi M (2013) Antioxidants: friends or foe in prevention or treatment of cancer: the debate of the century. *Toxicol Appl Pharmacol* 271:49–63. <https://doi.org/10.1016/j.taap.2013.05.004>
- Sayed AM, Hassanein EHM, Salem SH, Hussein OE, Mahmoud AM (2020) Flavonoids-mediated SIRT1 signaling activation in hepatic disorders. *Life Sci* 259:118173. <https://doi.org/10.1016/j.lfs.2020.118173>
- Schmiegelow K (2009) Advances in individual prediction of methotrexate toxicity: a review. *Br J Haematol* 146:489–503. <https://doi.org/10.1111/j.1365-2141.2009.07765.x>
- Shen F, Wang Z, Liu W, Liang Y (2018) Ethyl pyruvate can alleviate alcoholic liver disease through inhibiting Nrf2 signaling pathway. *Exp Ther Med* 15:4223–4228. <https://doi.org/10.3892/etm.2018.5925>
- Shin SM, Yang JH, Ki SH (2013) Role of the Nrf2-ARE pathway in liver diseases. *Oxidative Med Cell Longev* 2013:763257–763259. <https://doi.org/10.1155/2013/763257>
- Spurlock CF 3rd et al (2011) Increased sensitivity to apoptosis induced by methotrexate is mediated by JNK. *Arthritis Rheum* 63:2606–2616. <https://doi.org/10.1002/art.30457>
- Subramaniam SR, Ellis EM (2016) Umbelliferone and esculetin protect against N-nitrosodiethylamine-induced hepatotoxicity in rats. *Cell Biol Int* 40:761–769. <https://doi.org/10.1002/cbin.10611>
- Sun Y, Yuan X, Zhang F, Han Y, Chang X, Xu X, Li Y, Gao X (2017) Berberine ameliorates fatty acid-induced oxidative stress in human hepatoma cells. *Sci Rep* 7:11340. <https://doi.org/10.1038/s41598-017-11860-3>
- Tabassum H, Parvez S, Pasha ST, Banerjee BD, Raisuddin S (2010) Protective effect of lipoic acid against methotrexate-induced oxidative stress in liver mitochondria. *Food Chem Toxicol* 48:1973–1979. <https://doi.org/10.1016/j.fct.2010.04.047>
- Tait SW, Green DR (2013) Mitochondrial regulation of cell death. *Cold Spring Harb Perspect Biol* 5(9):a008706. <https://doi.org/10.1101/cshperspect.a008706>
- Trott O, Olson AJ (2010) AutoDock Vina: improving the speed and accuracy of docking with a new scoring function, efficient optimization, and multithreading. *J Comput Chem* 31:455–461. <https://doi.org/10.1002/jcc.21334>
- Tsai MS, Wang YH, Lai YY, Tsou HK, Liou GG, Ko JL, Wang SH (2018) Kaempferol protects against propacetamol-induced acute liver injury through CYP2E1 inactivation, UGT1A1 activation, and attenuation of oxidative stress, inflammation and apoptosis in mice. *Toxicol Lett* 290:97–109. <https://doi.org/10.1016/j.toxlet.2018.03.024>
- Wang X, Li R, Wang X, Fu Q, Ma S (2015) Umbelliferone ameliorates cerebral ischemia-reperfusion injury via upregulating the PPAR gamma expression and suppressing TXNIP/NLRP3 inflammasome. *Neurosci Lett* 600:182–187. <https://doi.org/10.1016/j.neulet.2015.06.016>
- Wu KC, Cui JY, Klaassen CD (2011) Beneficial role of Nrf2 in regulating NADPH generation and consumption. *Toxicol Sci* 123:590–600. <https://doi.org/10.1093/toxsci/kfr183>
- Yang Y, Kim SC, Yu T, Yi YS, Rhee MH, Sung GH, Yoo BC, Cho JY (2014) Functional roles of p38 mitogen-activated protein kinase in macrophage-mediated inflammatory responses. *Mediat Inflamm* 2014:352371–352313. <https://doi.org/10.1155/2014/352371>
- Yin J, Wang H, Lu G (2018) Umbelliferone alleviates hepatic injury in diabetic db/db mice via inhibiting inflammatory response and activating Nrf2-mediated antioxidant. *Biosci Rep* 38. <https://doi.org/10.1042/bsr20180444>
- Youle RJ, Strasser A (2008) The BCL-2 protein family: opposing activities that mediate cell death *Nature reviews*. *Nat Rev Mol Cell Biol* 9:47–59. <https://doi.org/10.1038/nrm2308>